ORIGINAL ARTICLE

Effect of complex shape of pier foundation exposure on time development of scour

Seung Oh Lee[1] · Irfan Abid[2] · Seung Ho Hong[3]

Abstract

Local pier scour has been recognized as one of the most significant causes of bridge failures. Despite numerous studies on the subject of local pier scour have been conducted, there remain problems in accurate scour prediction because almost of the past studies have focused only on scour depth around simple shape of a bridge pier with or without considering their time development, even though prototype bridges usually have complex pier configurations. Thus, the objective of this study is investigation of the scour process around complex shape of pier including various shape of foundations and columns other than cylindrical shape over time for the purpose of understanding the relationships between hydraulic variables and resulting time development of scour. In this study, two field sites in Georgia, USA were selected, and corresponding scale-down bridge models and river geometries were fabricated in a hydraulic laboratory to address objectives of this study. Three different sizes of sediment and several geometric scales of bridge pier models were used to investigate the effect of relative sediment size, which is defined as the ratio of the pier width to the median sediment size. Through the visualization experiment, it is observed that exposure of complex shape of pier footing has important role for the temporal variations of scour depth over time. In addition to the quantitative visualization analysis, based on the experimental results, scouring rate formulas are suggested with the help of dimensionless, effective flow work concept according to the value of the relative sediment size. Findings in this research can be used to improve scour prediction methods that currently tend to overpredict bridge scour depth.

Keywords Pier scour · Complex bridge configuration · Horseshoe vortex · Physical hydraulic modeling · Time development of scour

1 Introduction

Scouring around bridge foundations is the most common cause of bridge failures [1]. Historically, bridge failure results in loss of lives and huge financial losses for reconstruction and rehabilitation. In 1987, the collapse of the New York State Thruway

---

✉ Seung Ho Hong
    sehong@mail.wvu.edu

Extended author information available on the last page of the article

bridge resulted in the loss of ten lives. When a section of the US 51 bridge fell into the Hatchie River near Covington, Tennessee, eight people were killed in 1989. Six years later in 1995, seven people were killed due to the collapse of the Interstate 5 bridges over Arroyo Pasajero in California [2]. In the state of Georgia, during the 1994 floods, the increased flow scoured foundations and compromised infrastructure, causing the total failure of 31 state-owned bridges and the deaths of 28 people. Fifteen years later, flooding in 2009 resulted in the deaths of eight people [3]. Because of those two disasters during flooding in Georgia, total financial loss to the Georgia Department of Transportation (GDOT) was $130 million for the costs of replacing and repairing over 200 bridges that were damaged in 1994 [1] and again, the 2009 floods caused over $193 million in total damages [3].

Thus, to identify scour critical bridges and to ensure future bridge design guidelines properly accounting for increased intensity and frequency of rainfall events, numerous experimental as well as numerical studies have been conducted on scour around bridge piers [4–18]. However, unfortunately challenging problems still remain because of difficulties in understanding the complicated flow and the scouring mechanisms combined with complex geometries of bridge and various erodible bed materials [19]. Most of the past pier scour equations have focused only on simple shape of bridge pier with or without considering their time development, even though their time development around complex pier configurations including pier and pier bent should be examined to gain a more comprehensive understanding of realistic scour process.

As explained in the previous paragraph, time rate of local pier scour should be explored when the flow fields leading to scouring around bridge piers are investigated. Thus, in early studies, Carstens [20] proposed a dimensionless form of sediment-transport formula and applied it to scour around a vertical cylinder using similarity criteria for the temporal evolution of clear water scour which was based on a small range of laboratory-scale parameters. At the similar time, Shen et al. [21] tried to fit data into several combinations of parameters to develop time rate of scour. Later, Torsethaugen [22] conducted local scour experiments with wide diameter piers and suggested that time history of clear-water local scour on a polystyrene particle. However, their equations are not suited for practical application since they were constructed based on a narrow range of flow data [23].

In recent years, Zanke [24] proposed a semi-empirical formula for a temporal evolution of pier scour based on the principle of mass conservation on the bedload [25] and Dey [26] presented a theoretical model to estimate the time-variation of pier scour depth based on the conservation of the mass of sediment around circular piers mainly removed by horseshoe vortex system. Also, Ettema [27] studied time development of pier scour. He selected three dimensionless parameters, d_s/b, $u_* t/b$ and $\nu u_*/b$, to describe the similarity in the evolution of local scour depth with time where d_s is pier scour depth, b is the width of a bridge pier, u_* is the shear velocity, t is time, and ν is the viscosity. He compared temporal developments of scour depths by plotting, d_s/b versus $(d_s/b)(u_* t/b)(\nu u_*/b)$ at similar values of the relative sediment size parameter, b/d_{50}, where d_{50} is the median sediment size. In his plot, three segments were founded in which the first segment represented the rapid development of scour by downflow at the initial stage; the middle segment showed that scour depth developed as the horseshoe vortex moved away from the bridge pier and grew in strength; and the last segment represented the equilibrium scour depth [11]. Later, Melville and Chiew [9] proposed a method for determination of the time scale to develop the equilibrium scour depth, which was called an equilibrium time scale, and an equation for prediction of temporal development of local scour at cylindrical bridge piers in a uniform sand bed was given by

$$\frac{d_s}{d_{se}} = exp\left[-0.03\left(\frac{V_c}{V_1}\ln\left(\frac{t}{T_{eq}}\right)\right)^{1.6}\right] \tag{1}$$

where d_{se} is the equilibrium scour depth, V_1 is the mean approach velocity; V_c is the mean approach velocity at threshold conditions for sediment movement; T_{eq} is the time to reach the equilibrium scour depth. Their analysis was based on the extended laboratory data set obtained at the University of Auckland and the Nanyang Technological University, including Ettema's [27] and Graf's [28] experimental observations.

Oliveto and Hager [10, 29] summarized the laboratory data on abutment and pier scour conducted at ETH in Zurich, Switzerland and found the effect of the densimetric particle Froude number (Fr_d) on time development of scour depth as defined by Eq. (2)

$$Fr_d = \frac{V_1}{\sqrt{g'd_{50}}} \tag{2}$$

where g' is the reduced gravitational acceleration ($=\left[(\rho_s - \rho)/\rho\right]g$, in which ρ_s and ρ is the density of sediment and water, respectively). Further research by Kothyari et al. [30] suggested that time development of scour is mainly influenced by the densimetric particle Froude number as well as geometrical effect which is the width and the shape of a pier or an abutment. Recently, Chang et al. [31] and Kothyari and Kumar [32] conducted laboratory experiments to find the temporal variation of scour around a circular cylinder and Lanca et al. [33] investigated the impact of sediment coarseness around large cylindrical piers. Based on the findings by several researchers, the rate of scour development is strongly related to the approach flow velocity and sediment size, which can be comprehensively represented by the flow intensity [34, 35]. More recently, the effect of unsteady flow conditions on the temporal evolution of a pier scour have been studied. Link et al. [36] proposed mathematical model, dimensionless, effective flow work (DFW) based model, W^* to explore time development of pier scour under unsteady flow conditions imposed by hydrographs as follows

$$W^* = \int_0^{t_{end}} \frac{1}{t_R}\left(\frac{V_1 - 0.5V_c}{V_R}\right)^4 \delta dt \tag{3}$$

$$Z^* = f\left(d^*, \rho', \frac{y_1}{d_{50}}, \frac{b}{d_{50}}, W^*\right) \tag{4}$$

where W^* is dimensionless, effective flow work, t_{end} is time for end of scouring, t_R is the reference time (d_R/V_R), in which d_R is the reference length ($b^2/2d_{50}$) and V_R is the reference velocity $\left(\sqrt{\frac{\rho_s - \rho}{\rho}gd_{50}}\right)$. $Z^* = d_s/d_R$ is normalized scour depth, d^* is dimensionless sediment diameter $\left(\frac{\rho'g}{\gamma^2}\right)^{1/3}d_{50}$, ρ' is the relative density $\left(\frac{\rho_s - \rho}{\rho}\right)$.

Further studies by Pizarro et al. [37] introduced bridge-pier scour entropic (BRISENT) model based on both the informational entropy concept and the principle of maximum entropy. Both of DFW and BRISENT model successfully reproduced time development of scour evolution with high accuracy under steady hydraulic conditions, step-wise hydrographs and unsteady flood waves [25]. Although the researches mentioned in the previous paragraphs successfully considered time development of local

scour under steady/unsteady hydraulic conditions, most of the proposed formulas are derived based on the experiments conducted with a simple shape of pier in a straight rectangular channel even though most of prototype bridge foundations have complex pier bent geometry including shapes other than cylindrical, multiple columns with variable spacing along the pier column, and multiple pier bents at variable flow depths across a river.

With the help of well-controlled laboratory experiment, the effects of selected flow parameters around a bridge pier have been examined. However, due to the difficulty in reproducing prototype local scour depths utilizing laboratory model experiments, the scaling procedure must be carefully considered when comparing laboratory data with prototype data. In addition, the need for using the appropriate nondimensional parameters is essential when laboratory experiments are designed and conducted so that the nondimensionalized results can be compared with field data. Raudkivi [38] discussed the functional trends of the pier scour with three important nondimensional parameters; V_1/V_c: effect of flow intensity, y_1/b: effect of flow depth where y_1 is the approach water depth, and b/d_{50}: effect of relative sediment size. It is shown that the initiation of sediment motion around a pier scour under clear water condition is placed between $V_1/V_c = 0.4$ and 0.5. Thus, in general, clear water scour regime can be defined for $0.5 \leq V_1/V_c \leq 1.0$ [34–36], where the scour depth increases almost linearly with increasing V_1/V_c. Scour depth fluctuate with time due to incoming sediment and the passage of bedforms through the scour hole for $V_1/V_c \geq 1.0$, which is live-bed scour regime. As a result, the scour depth is considered to be independent of flow intensity under live-bed scour conditions [8]. More recent study by Sheppard and Miller [39] shows that the pier scour depth increased as V_1/V_c increases in live-bed scour regime and reached peak at "live-bed peak velocity".

For the effect of flow depth, when the flow depth increases, the interference of the surface roller formed ahead of the bridge pier with the downflow and horseshoe vortex is reduced, and the effect of flow depth becomes independent when $y_1/b > 3.0$ [31]. Later, several other researchers [25, 36, 40] observed similar findings in their experiments with different criteria. In the field, the effect of sediment size is not important because the value of b/d_{50} is large enough not to affect the scour depth [38]. However, in the laboratory, the equilibrium scour depth tends to decrease with smaller b/d_{50} and be independent of the ratio when b/d_{50} is greater than 25 [41] or 50 [9, 12] based on laboratory results; thus, the effect of sediment size can be one of the most significant parameters in laboratory experiments [38, 42]. Sheppard et al. [12] and Lee and Sturm [42] have suggested that relative scour depth may also decrease at very large values of $b/d_{50} > 25$ based on experiments in a very large flume.

Now-a-days, because of geotechnical, structural and economic considerations, complex pier bent geometry is preferred over simple piers in bridge construction. Thus, several researchers [44–47] conducted laboratory studies using complex shape of pier foundation, recently. However, they [44–47] have only focused on the flow structure around the foundation leading to the resulting equilibrium scour depth without consideration of time. In this study, the main objective is to provide a better understanding of pier scour process over time in various pier foundation geometries under different sediment size. To investigate time development of scour around complex configuration of pier bent, physical laboratory experiments were conducted using flat-bed model as well as scale down physical river model. Using acoustic Doppler velocimeter (ADV), velocities and bed elevations are measured before scour, during scour process at specified intervals, and after equilibrium scour.

In addition to the velocity flow field and the scour depth measurements with the ADV, scour process over time is recorded with high-speed camera.

2 Methods

Local scouring around a pier is a consequence of the intricate interactions of many parameters, therefore it is recommended that the effect of each parameter needs to be investigated individually through dimensional analysis. The resulting dimensional analysis for local pier scour depth is as following [9, 27]:

$$\frac{d_s}{b} = f\left(Fr_1, Re, \frac{y_1}{b}, \frac{V_1}{V_c}, \frac{b}{d_{50}}, \frac{tV_c}{y_1}\right) \tag{5}$$

Fr_1 is approach Froude number that governs open channel flow through the bridge and Re is Reynolds number which can be negligible around the pier because of fully-turbulent flow conditions. The relative scour depth, d_s/b, can be physically implicated as the scouring that is due to the horseshoe vortex system, which is a function of pier width, b. The effect of approach flow depth is expressed by y_1/b. It represents the relative influence of the depth of flow and the size of the horseshoe vortex as reflected by b. The mobility of bed materials for scouring is expressed by V_1/V_c which is called the flow intensity. b/d_{50} shows the effect of relative sediment size. For rough bed flow, the exchange of momentum in the boundary layer is generally controlled by the bed roughness rather than the fluid viscosity [48, 49]. The horseshoe vortex system and the distance to the separation point upstream of the pier are influenced by the bed roughness related to the sediment size. For larger sediment size, the momentum of the downflow at the upstream edge of the pier is more dissipated than for smaller sediment sizes due to bed porosity. With increasing values of b/d_{50} up to a certain threshold, a larger and stronger horseshoe vortex system is expected since the momentum exchange is decreasing, thus the scour depth is also increasing. Finally, the time scale can be defined as tV_c/y_1 to show the development of scour depth in front of a pier [50, 51].

2.1 Experimental setup

All experiments were conducted in the hydraulics laboratory of the School of Civil and Environmental Engineering at the Georgia Institute of Technology, Atlanta. To replicate actual bridge pier model and river geometries in the laboratory, two field sites in Georgia (Chattahoochee River Bridge and Flint River Bridge) were selected and corresponding bridge geometries and river bathymetries were received from GDOT and United State Geological Services (USGS), respectively [52]. As shown in Fig. 1a, Chattahoochee River Bridge pier bent consists of four rectangular concrete columns and rectangular concrete footings. The bridge piers were designed to be aligned with the flow. The pier width of the most upstream pier is 1.07 m. The drainage area is 816 km^2 and the shape of cross-section has compound channel which include approximately 70 m wide of main channel and floodplains on both side of the river. The channel at this site is straight for several hundred meters upstream and downstream of the bridge. Total eleven cross-sections were surveyed including upstream and downstream of the bridge to construct

(a)

(b)

Fig. 1 Bridge over: **a** chattahoochee River and **b** Flint River

the river bathymetry for physical modeling and collected bed material samples from the site shows that the median size of bed material around the center of the channel is about 0.7 mm and the geometric standard deviation is 1.6. For Flint River bridge, each pier bent has two square concrete pier columns placed on large stepped square concrete footings as shown in Fig. 1b. The upstream pier column width is 1.83 m. The drainage area for the site is 19,606 km^2 and the width of the main channel is approximately 150 m and there is a very wide and flat floodplain on both sides of the main channel. The channel is straight for hundreds of meters upstream and has a sharp bend about 150 m downstream of the bridge. The peak discharge at the bridge site was recorded as 3058 m^3/s on July 14, 1994 during tropical storm Alberto, which was greater than the 100-year flood. Five cross-sections were surveyed throughout the channel reach for physical modeling and the sediment particle size distribution of a bed material sample collected on the upstream side of the bridge site shows that the median size of the bed material sample

is approximately 0.4 mm and the geometric standard deviation is 2.17. More detailed schematic of each bridge pier along with the prototype dimensions, shape of each surveyed cross-sections shape and measured particle distributions of each site can be found in Sturm et al. [52] and Lee and Hong [53].

The bridge pier models and surveyed river bathymetries were fabricated with wood, acrylic, and aluminum plates, and built inside a 4.3 m wide by 24.4 m long horizontal flume. Two different experimental scenarios were simulated in the horizontal flume. First, flat-bed (FB) experiments were conducted to investigate the effect of individual parameters and interaction among parameters that affect scour around the main pier bent. Second, in river-bed (RB) model, experiments were operated with the full flume width of 4.3 m in which the complete river bathymetry upstream and downstream of the bridge as well as the embankments, abutments, and pier bents of the bridge itself were modeled in detail. Thus, for the river model, the length scale ratio, shown in Table 1, was determined by the comparing measured field extent with physical horizontal flume space. Additional length scale ratios for the flat bed model were selected by following modeling guideline to find the effect of b/d_{50} on time development of pier scour.

One of the basic physical modeling strategies is that Froude number similarity and the geometric similarity (y_1/b) are maintained between the prototype and laboratory modeling while selecting the sediment size such that clear water scour was obtained ($0.5 \leq V_1/V_c \leq 1.0$) in the laboratory. Thus, three different sizes of sediments (3.3 mm, 1.1 mm, and 0.53 mm) were selected for this study. Even if for the most of cases has the $b/d_{50} \geq 25$, several cases for the flat bed model were conducted under $b/d_{50} < 25$ to find the effect of b/d_{50} on the time development of scour around complex shape of pier. Then, as shown in Table 2, possible experimental runs (discharge and water depth) were selected from measured hydrograph provided by USGS and basic flow variables were decided based on the Froude number similarity to satisfy the conditions of $0.5 \leq V_1/V_c \leq 1.0$ and $y_1/b > 3.0$ in the laboratory to conduct the experiment in clear-water scour regime.

For the flat-bed experiment, an interior channel width of 2.4 m was constructed by installing concrete blocks as interior walls of the entire flume and the main pier bent of each bridge was modeled individually in the channel with a movable sediment bed that was initially leveled to form a horizontal or flat-bed prior to the beginning of scour. Also, during the flat-bed experiments, calibration and uncertainty of the instruments and experimental procedure were investigated by comparison of repeated experiments. In river-bed (RB) model, based on river bathymetry data from the USGS, the river model was fabricated with a proper length scale to fit the horizontal flume. All cross sections were built with plywood templates cut according to the USGS field survey. Bridge pier geometry and location as well as bridge abutments and embankments were modeled

Table 1 Bridge model scales, pier shape, and pier width

Model	Scale	Pier shape	Pier width in model (m)	Pier width in field (m)	Remark
Chattahoochee River	1:23	Rectangular	0.046	1.067	FB, VE
Chattahoochee River	1:40	Rectangular	0.027	1.067	FB, RB
Flint River	1:33	Square	0.055	1.829	FB, VE
Flint River	1:50	Square	0.037	1.829	FB, RB
Flint River	1:90	Square	0.021	1.829	FB

FB flat-bed experiment, *RB* river model experiment, *VE* visualization experiment

Table 2 Experimental conditions and summary of dimensionless experimental data for the Chattahoochee River models and Flint River model

River	Run	Model	Scale	Q (m³/s)	d_{50} (mm)	b (m)	T_{eq} (h)	y_1/b	V_1/V_c	b/d_{50}
CH	1	FB	1/23	0.238	3.3	0.046	32	4.16	0.70	13.95
	2	FB	1/23	0.273	3.3	0.046	36	4.16	0.76	13.95
	3	FB	1/23	0.289	3.3	0.046	36	4.16	0.83	13.95
	4	FB	1/23	0.289	3.3	0.046	37	3.33	1.07	13.95
	5	FB	1/40	0.03	0.53	0.027	28	3.96	0.90	50.92
	6	FB	1/23	0.051	0.53	0.046	30	4.16	0.85	86.84
	7	FB	1/23	0.044	0.53	0.046	12	3.09	1.01	86.84
	8	RB	1/40	0.127	3.3	0.027	48	7.09	0.76	8.18
	9	RB	1/40	0.142	3.3	0.027	48	7.09	0.82	8.18
	10	RB	1/40	0.069	3.3	0.027	48	4.02	0.82	8.18
	11	RB	1/40	0.068	3.3	0.027	48	4.02	0.84	8.18
	12	RB	1/40	0.071	1.1	0.027	48	7.04	0.71	24.53
	13	RB	1/40	0.038	1.1	0.027	47	3.95	0.75	24.53
	14	RB	1/40	0.085	1.1	0.027	47	7.04	0.78	24.53
	15	RB	1/40	0.042	1.1	0.027	47	3.95	0.83	24.53
	16	RB	1/40	0.047	1.1	0.027	47	3.95	1.00	24.53
FL	17	FB	1/50	0.219	3.30	0.037	48	4.38	0.70	11.2
	18	FB	1/50	0.218	3.30	0.037	48	4.17	0.75	11.2
	19	FB	1/50	0.251	3.30	0.037	48	4.33	0.77	11.2
	20	FB	1/50	0.283	3.30	0.037	48	4.50	0.88	11.2
	21	FB	1/90	0.026	0.53	0.021	43	6.18	0.64	39.1
	22	FB	1/90	0.033	0.53	0.021	24	6.18	0.80	39.1
	23	FB	1/50	0.042	0.53	0.037	28	4.08	0.87	69.0
	24	FB	1/50	0.079	0.53	0.037	12	6.18	1.07	69.0
	25	FB	1/33	0.054	0.53	0.055	48	4.35	0.67	105
	26	FB	1/33	0.052	0.53	0.055	24	3.07	0.91	105
	27	RB	1/90	0.042	1.10	0.021	48	7.35	0.57	19.1
	28	RB	1/90	0.047	1.10	0.021	96	7.35	0.67	19.1
	29	RB	1/90	0.051	1.10	0.021	96	7.35	0.78	19.1

CH Chattahoochee River, *FL* Flint River

according to bridge plans provided by the GDOT and the GPS positions measured in the field by the USGS. For establishing uniform flow as the inlet flow condition, the upstream river cross section in RB model was duplicated and installed with a horizontal spacing of approximately 1.5 m to provide an approach prismatic channel of length equal to at least forty-five flow depths. Then, the entire spaces between the templates including test section and approach section were filled with bed sediment and carefully leveled to the elevations established by the templates. In addition to the experiments in horizontal flume, several cases were simulated in a 1.1 m wide by 24.4 m long rectangular glass sided tilting flume for detailed visualization experiments (VE) with high speed camera. The camera can achieve up to 120 frames per second (fps) with a resolution of 460×480 pixels.
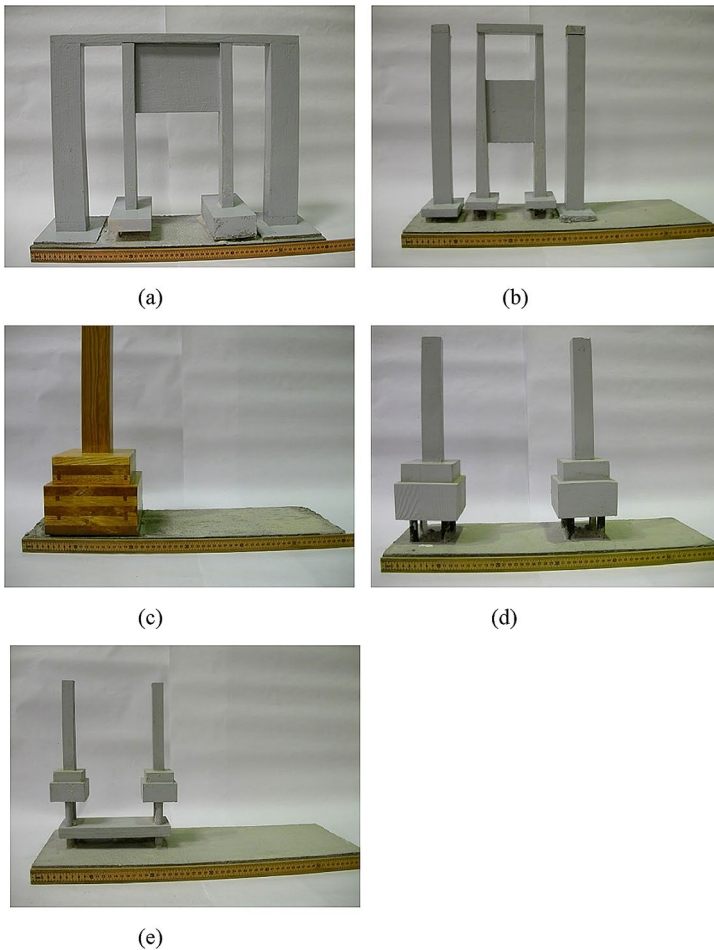
Fig. 2 Bridge models for this study: **a** Bridge pier in Chattahoochee River model with 1:23 scale, **b** Bridge pier in Chattahoochee River model with 1:40 scale, **c** Bridge pier in Flint River model with 1:33, **d** Bridge pier in Flint River model with 1:50 scale, and **e** Bridge pier in Flint River with 1:90 scale

Table 1 and Fig. 2 show five bridge pier models with individual scales for this study decided by the criteria as explained in above paragraphs. Figures 3 and 4 show the example case of river-bed model for Chattahoochee River and Flint River, respectively and Fig. 5 is initial setting of flat-bed model using 1:23 scale down Chattahoochee River bridge pier.

2.2 Experimental procedure

After completion of laboratory setup, the flume was filled with water for an experiment from a downstream supply hose at a very slow rate so that the sand would be saturated safely and remain undisturbed. After complete saturation, a required discharge was established using a magnetic flowmeter with flow depth adjusted well above the required value

(a) Bridge section looking downstream
from the right bank

(b) Bridge section with embankment
looking downstream for the left floodplain

Fig. 3 River-bed model for Chattahoochee River

(a) Bridge section looking downstream from the left bank

(b) Railroad bridge looking downstre to highway bridgeam

Fig. 4 River-bed model for Flint River

Fig. 5 Flat-bed model for Chattahoochee River bridge

by using the tailgate. Then the flow depth was gradually decreased by changing the height of the tailgate until the target approach flow depth was obtained. During this time, the point gage on the instrument carriage was used to monitor the flow depth. Once the target flow-rate and the flow depth had been reached, vertical profiles of point velocities were measured at the approach point located ten pier widths upstream of the face of the pier using the ADV. The upstream flow approach points where there is no effect of the existence of bridge piers on the velocity profile was determined by comparing velocity profiles measured upstream of the main bridge pier at different positions along the pier centerline.

During each experimental run, temporal change of bed elevations in front of a bridge pier was measured periodically using the ADV temporarily positioned for a moment above the point of scouring. At the completion of each experiment, the final bed elevations were measured in the same way as the initial elevations using the ADV and the point gage. During measurement of bed elevations with the ADV, the flume was not fully drained because the ADV probe needed to be completely submerged. After finishing with the bed elevation measurements with the ADV, the flume was slowly drained so as not to disturb the scour contours and the final bed elevations near a bridge pier or footing were measured with the point gage. The closing time of the experiment was determined when the local scour depth reached the equilibrium state at which there were negligible changes in bed elevation with time as guided by Melville and Chiew [9], but it was never less than 48 h. When one experiment was completed, the moveable bed had been re-leveled according to the templates installed in the test section, the templates were carefully removed and the bed elevations were measured in detail throughout the test section with a horizontal spacing of approximately 0.06 m to set-up initial bed contours before each experiment.

3 Results and discussion

As shown in Table 2, total twenty-nine experiments were conducted for this research and the experimental conditions have been summarized in terms of dimensionless parameters include relative flow depth (y_1/b), flow intensity (V_1/V_c), relative sediment size (b/d_{50}) as expressed in Eq. (5). The critical velocity of the initiation of sediment motion, V_c, was calculated from Keulegen's equation. The ranges of dimensionless parameters in Table 2 are

the result of the experiments using different scale of models in flat-bed (FB) and river-bed (RB). In general, the value of y_1/b was controlled to agree either with the bankfull value of approximately 4.0 or the 100-year flood value of approximately 7.0 based on the field measurements.

3.1 Temporal variation of local scour depth around complex bridge foundation

Local scour depth at the nose of the bridge pier was recorded with the ADV over time throughout the experiments. Selected temporal variations of the local scour depth for each experiment in the Chattahoochee River model and in the Flint River model are plotted on the semi-logarithmic scale in Fig. 6. As shown in Fig. 6a, all scour depths observed both in the flat-bed and river-bed experiments for Chattahoochee River rapidly changed at the initial stage and the rate of scouring became smaller with time. Finally, the scour depth reached the equilibrium state, which is similar findings by other researchers. However, for the case of Flint River model, the bed elevation at the initial stage showed stagnation and then, was rather gradually followed by a more rapid increase. To understand and to compare the unique shape of time development of the scouring between Chattahoochee River bridge model and Flint River bridge model, additional flat-bed experiments were conducted in a glass sided tilting flume, and the time evolutions of scour were captured by high-speed camera. Figures 7 and 8 shows the selected example. As shown in Fig. 7, the initial scouring began in the vicinity of the pier and then the two conical scour holes merged at the center of the nose of the pier for the Chattahoochee River model. This process dominated by the flow occurred within only 9 s. After merging, the horseshoe vortex became the main agent to carry away the sediment from front of the pier. The scour depth became deeper with the time and after reaching the equilibrium state, the rate of scouring became too small to be measured during at least 3 h. However, for the Flint River bridge as shown in Fig. 8, two conical scour holes developed at both edges of the footing in the early stages of development and moved upstream until they converged at the nose of the footing. After convergence, scour depth increased more rapidly as shown in experimental Run 18 in Fig. 6b. In the other three experiments in Fig. 6b, the retardation of the developing scour depth was observed to occur in a comparably shorter time period due to the approach flow velocity and sediment size. The subsequent slopes of the scour development with time at the nose of the footing depended on the approach flow velocity and sediment size and will be discussed in more detail in next sub-chapter.

As shown in Fig. 8, the tops of the footings in the Flint River model are already exposed at the beginning of scour because of degradation over time or previous flooding events in the field; that is, the elevation of the top of the upper footing is about the same as the bed elevation near the footing. Typically, the effect of an exposed footing is to reduce the rate of local scour due to interception of the downflow feeding the horseshoe vortex upstream of the pier [6, 54, 55]. Another remarkable feature in the temporal variation of the scour depth around the footing of the Flint River bridge is that a mild slope is observed in the middle of the scour process for some experiments due to the exposure of the step footing (see Figs. 2c–e, 6b). After the scour hole reached the nose of the footing, the scour depth increased at a constant rate of change until the bed elevation reached the elevation of the second footing. Then development of the scour depth slowed as shown in flat-bed experimental Run 24 and river-bed experimental Run 29 as the flow structure and strength of the
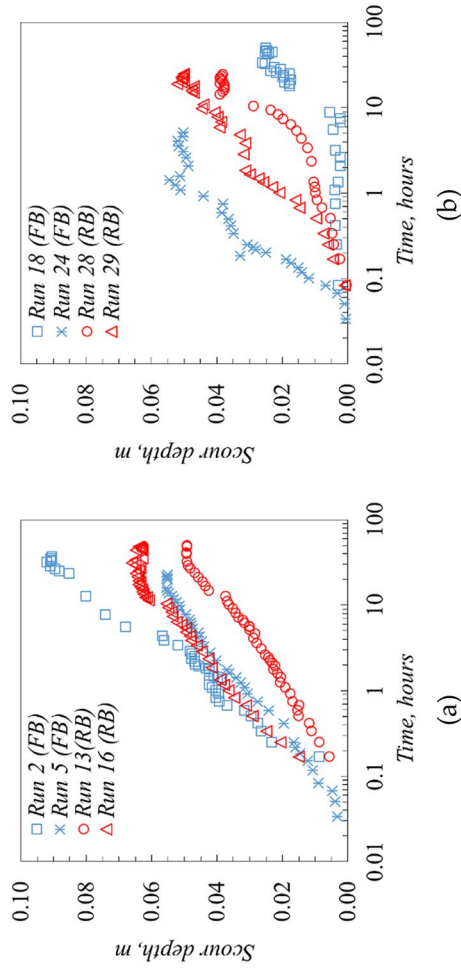
Fig. 6 Selected temporal development of scour depth for **a** Chattahoochee River Model and for **b** Flint River Model

Fig. 7 Temporal variation of scour depth at nose of the pier using CH bridge model (Scale = 1:23, $V_1/V_c = 0.85$, $y_1/b = 4.16$, $b/d_{50} = 86.84$; same hydraulic condition as in Run 6)
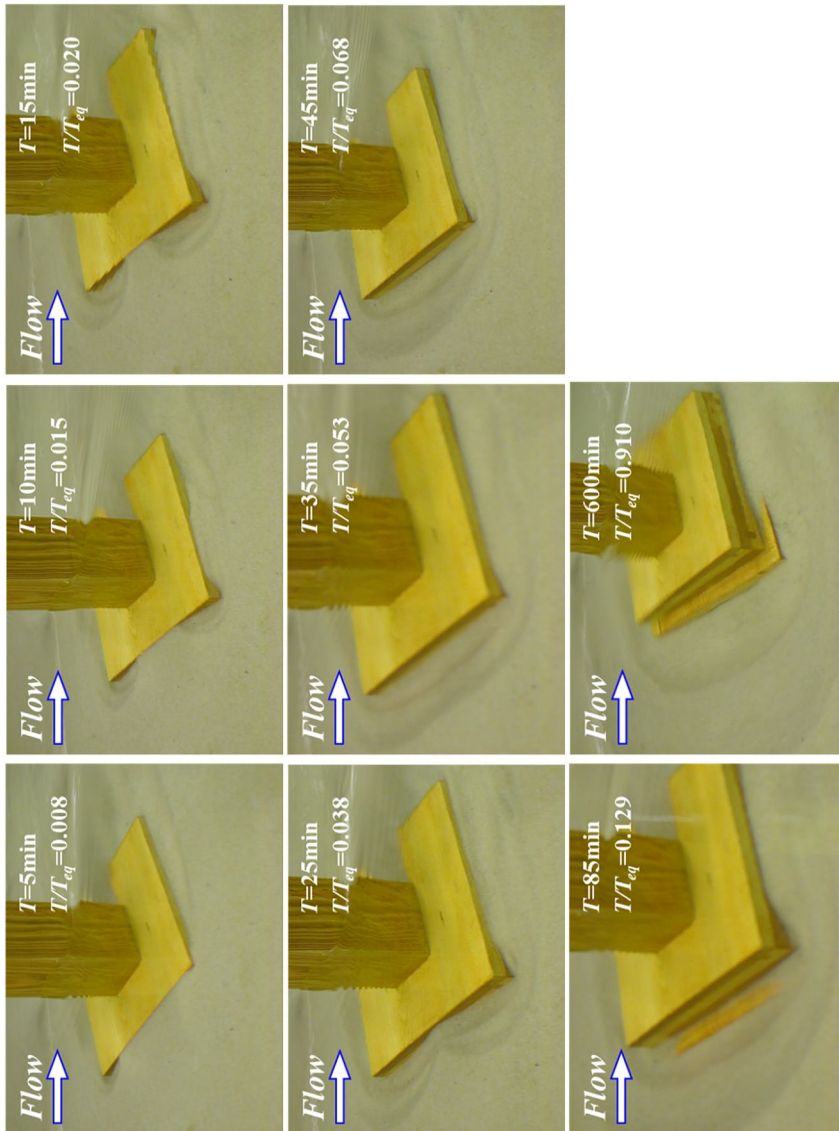
Fig. 8 Temporal variation of scour depth at nose of the pier using FL bridge model (Scale = 1:33, $V_1/V_c = 0.91$, $y_1/b = 3.07$, $b/d_{50} = 105$; same hydraulic condition as in Run 26)

horseshoe vortex changed due to the new geometry. Afterward, scour began increasing at a higher rate followed by the asymptotic approach to the equilibrium state.

3.2 Effect of flow intensity and relative sediment size on temporal variation of local scour depth

Figure 9a, b show selected runs of time development of scour depth in terms of non-dimensionless variables for flat-bed experiment and river-bed experiments, respectively, in the Chattahoochee River model. Each experimental condition in Fig. 9a, b, respectively, were conducted with same value of y_1/b and b/d_{50}, but under different V_1/V_c so that the effect of flow intensity on time development of scour could be examined. As shown in Fig. 9, the slope of each curve is clearly dependent on the flow intensity with the slope increasing with increasing flow intensity. The equilibrium time, T_{eq}, is independent on the flow intensity in both the flat-bed experiments and the river-bed experiments. Observations from Fig. 9 suggest that the equilibrium time is independent of flow intensity when the development of scouring is monitored at the nose of a pier in agreement with Melville and Chiew [9] 's data.

However, for the Flint River model, different time development scenario is observed due to the complex shape of bridge foundation and their exposure. As explained in the previous chapter, the exposed pier footing caused some delay in scour hole development. Since the surface elevation of the footing was about the same as the initial bed elevation at the central bridge pier bent for the Flint River bridge, the development of the scour depth started first at both sides (corners) of the footing due to the flow of the horseshoe vortex wrapping around the pier. Two conical-shaped scour holes were detected in the vicinity of the footing on either side as shown previously in Fig. 8. When the two conical scour holes at both sides became larger and then met eventually at the nose of the first pier footing, the local scour depth at the nose of the pier footing started developing. That starting stage is used as the beginning time of the scour depth at the nose of the pier in the Flint River modeling in Fig. 10. The beginning time is dependent on the flow intensity. It took longer for the scour hole to begin development at the nose of the pier footing for smaller flow intensity. However, the slopes from the regression analysis are approximately the same for different flow intensities in the flat-bed experiments. A similar result was obtained in the river-bed experiments. The strength of the horseshoe vortex system in front of the footing is less than that in front of the pier since the role of the downflow along the upstream face of the pier becomes significantly smaller in the former case. Therefore, the rate of scouring is less dependent on the flow intensity so that the slopes in Fig. 10 are comparable.

The effect of relative sediment size is also examined by comparing experiments with approximately the same values of the flow intensity and the relative flow depth, and the dimensionless effective flow work introduced by Link et al. [36] and Pizarro et al. [56]. It was difficult to obtain exact comparisons, but for example, the relative differences in flow intensity and relative flow depth were within 10% between experimental Run 4 and Run 7 in the Chattahoochee River model. Hence, those cases were selected to study the effect of the relative sediment size alone as shown in Fig. 11. As shown in Fig. 11, the equilibrium time, T_{eq}, is highly affected by the relative sediment size, b/d_{50}, in the clear-water condition. When the value of b/d_{50} increased, the value of T_{eq} is reduced since the reduction of the sediment size decreases the critical velocity [57]. Decreasing the critical velocity requires the approach velocity to become smaller to match the same flow intensity, V_1/V_c. If the strength of the horseshoe vortex system is mainly dependent on the pier size and flow
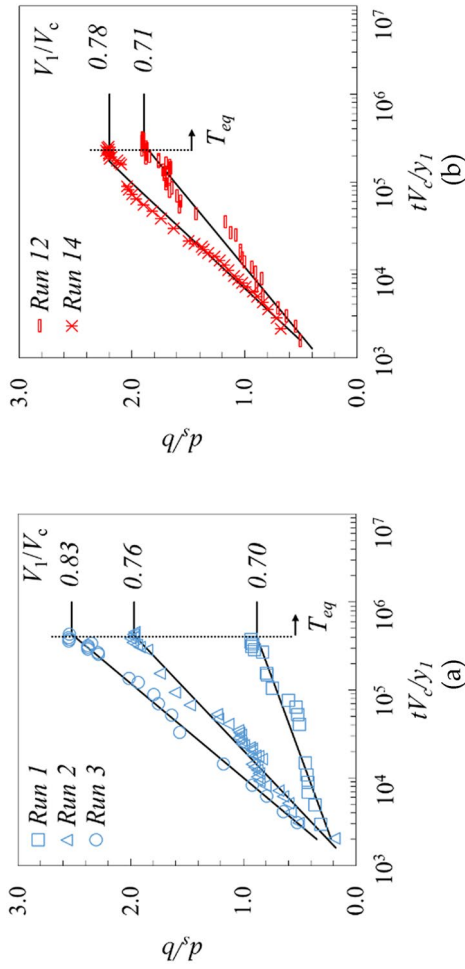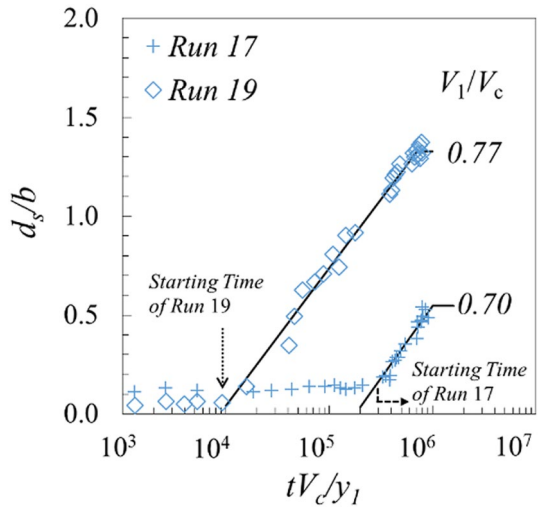
Fig. 9 Comparison of temporal development of scour depth for **a** flat-bed model (Scale 1:23, $y_1/b = 4.2$, $b/d_{50} = 13.95$) and **b** river model (Scale 1:40, $y_1/b = 7.0$, $b/d_{50} = 24.5$) in Chattahoochee River

Fig. 10 Comparison of temporal development of scour depth in the Flint River model (Scale 1:50, $y_1/b = 4.3$, $b/d_{50} = 11.1$)

condition, then so is the equilibrium time [58–60]. Thus, the equilibrium time with small sediment is less than that with large sediment when other conditions are the same.

Further investigation of the effect of sediment size or b/d_{50} on the time development of scour is conducted by using the dimensionless effective flow concept, describe in Eqs. (3) and (4). As shown in Eq. (4), normalized scour depth (Z^*) is function of several non-dimensional variables. Because relative sediment density, ρ', was constant in all experiment and the relative flow depth ($y_1/d_{50} \geq 150$) can be assumed large enough not to affect the scour depth, remaining variables, dimensionless sediment diameter (d^*), b/d_{50}, and dimensionless effective flow (W^*) was considered for further analysis. Figure 12 show the time development of dimensionless form of pier scour depth for FB model and RB model of Chattahoochee River and Flint River model, in terms of dimensionless form, W^*, and b/d_{50} and d^* as third and fourth parameter. The Z^* follows a linear trend with the logarithm of the W^* (average R^2 is 0.98), and then reaches equilibrium after a certain time for Chattahoochee River model. Furthermore, Fig. 12a, b shows that different flow conditions (different experimental runs) produced the same relative scour depth for given values of W^* when the comparison is conducted with the experimental runs having same value of b/d_{50}, leading to the uniqueness of the relation between both variables, and demonstrating that W^* is an appropriate parameter for delineating time development of pier scour as suggested by Link et al. [61]. However, for the case of Flint River model shown in Fig. 12c, because of the complex shape of bridge foundation and exposure of the step footing for some cases of experimental runs, unique relationship cannot be found. The most probable cause for these differing scenarios in the Flint River model is flow structure and strength of the horseshoe vortex, which is main driver of the pier scour, is changed when they encountered with the new geometry which was originally founded deeply under the sediment bed.

It is interesting to note that the observations from Fig. 12a, b suggest that the slope of the time development of normalized scour depth is a unique function of b/d_{50}. The best-fit regression analysis for the value of Z^* and W^* ($R^2 > 0.95$ for all of the cases) in Fig. 12a, b were used to calculate scouring rate and the regression line with respect to each value of b/d_{50} was included in Fig. 12a, b. As shown in Fig. 12a, b, when the value of b/d_{50} increased, the rate of scouring decreased. As the sediment size decreased (b/d_{50} increased),
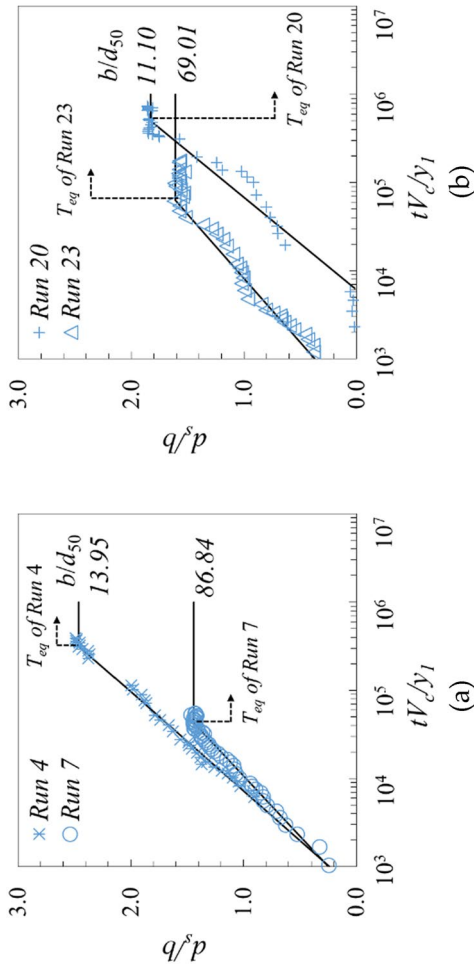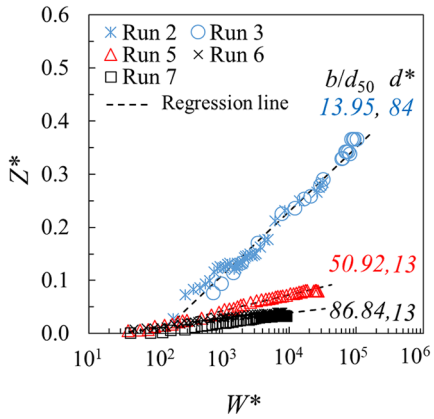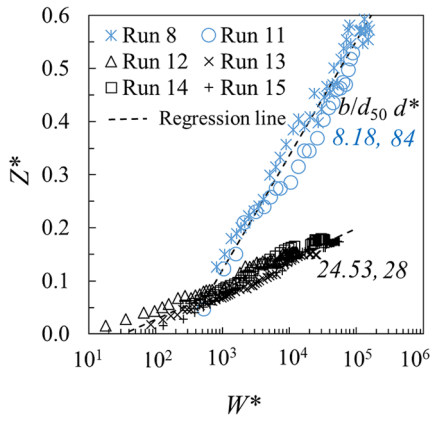
Fig. 11 Effect of b/d_{50} on temporal development of scour depth for **a** CH bridge model (Scale 1:23, $y_1/b \approx 3.1$, $V_1/V_c \approx 1.0$) and **b** FL bridge model (Scale 1:50, $y_1/b \approx 4.3$, $V_1/V_c \approx 0.9$)
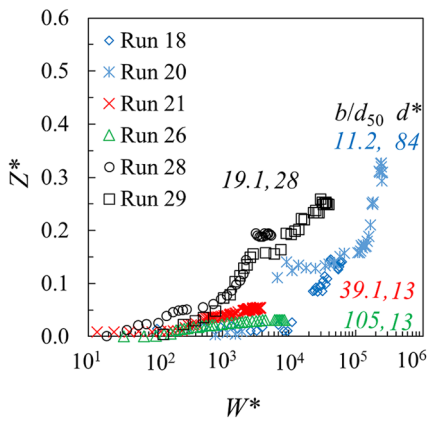
Fig. 12 Effect of b/d_{50} on the time development of scour depth in dimensionless form (Z^*) with W^* for **a** flat-bed model for Chattahoochee River, **b** river-bed model for Chattahoochee River, and **c** Flint River model
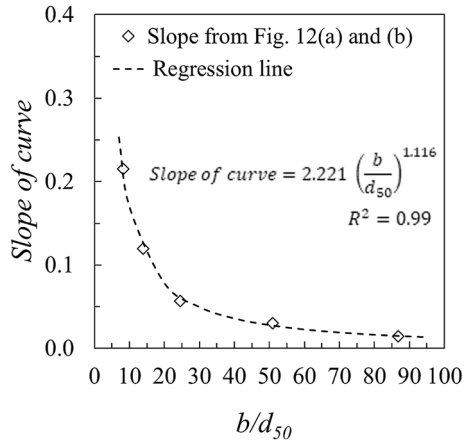
the critical velocity is also decreased. Similar reasoning as for the T_{eq}, when the critical velocity decreased, the approach velocity becomes smaller under the same flow intensity, V_1/V_c, leading to the reduced strength of the horseshoe vortex system. Thus, the rate of scouring becomes smaller. Based on the findings, Fig. 13 shows the unique relationship between the rate of scouring (the slope of curve) and the value of b/d_{50}. Because of additional factors required for additional study including exposure time of footing and the effect of their size, the results from the Flint River model are not included for the analysis. As shown in Fig. 12, dimensionless sediment diameter (d^*) is not related with the time development of pier scour in this study, but the determination of a more accurate picture of the complex flow physics and the resulting sediment transport around an complex shape of pier calls for additional experiments under various value of b/d_{50} and d^*.

4 Conclusions

An analysis of existing pier scour formulas indicates that most methods overestimate scour depth around bridge foundation. Deficiency of measured laboratory data conducted with using realistic geometry and/or field data availability can be one of the most important factors. In addition to data deficiency, current engineering practice of using equilibrium scour depth can be another factor because the equilibrium scour depth may serve as only a conservative estimate of prototype scour unless the effect of time is taken into account. Furthermore, complex shape of pier foundation can get exposed during flooding, which poses a challenge to the engineers in prediction of scour depth because of generating new vortex structure around the foundation leading to unexpected scour depth. Under these circumstances, to attain a more thorough understanding of the complex flow physics and resulting time development of sediment transport around a realistic shape of pier, scaled physical model studies were conducted using actual river bathymetries and pier geometries in the hydraulic laboratory, and the results are analyzed in terms of non-dimensional variables; flow intensity (V_1/V_c), relative sediment size, b/d_{50}, and relative approach flow depth, y_1/b as well as dimensionless, effective flow work (DFW) based model, W^*. The experimental results shows that the relative scour depth, defined as the ratio of scour depth to width of a pier, follows a linear trend with the logarithm of the dimensionless time scale, and the

scouring rate (slope) is clearly dependent on the flow intensity when the pier footing is deeply embedded. However, when a pier foundation is exposed, because the pier foundation intercept downflow which is a main driver feeding horseshoe vortex upstream of the pier, the time rate of scour is not related to the flow intensity. In addition to the effect of flow intensity, the time for equilibrium scour depth itself is highly influenced by the value of b/d_{50}. For further analysis using DFW based model, relative scour depth shows unique relationships with the value of W^*, demonstrating that W^* is an appropriate parameter for delineating time development of pier scour when the pier is not exposed. Based on the results, formulas for the "rate of scouring" are suggested with respect to the value of b/d_{50} for the case when the pier footing is not exposed, which calls for additional experiments under various flow and geometries conditions, but in the other hands, which has great promise for the future application of sophisticated CFD (Computational Fluid Dynamics) to explore mechanism of sediment transport over time around a bridge foundation. Even if this study provides qualitative insights into the characteristics of time development of pier scour around complex bridge foundation with and without their exposure, the effect of relative sediment size, b/d_{50} deserves further study because it should be understood either for predicting scour depths or selecting the appropriate sediment size in physical models of scour.

References

1. Arneson LA, Zevenbergen LW, Lagasse PF, Clopper PE (2012) Hydraulic Engineering Circular No. 18 (HEC-18): Evaluating scour at bridges, 5th edn
2. Miller W (2003) Model for the time rate of local sediment scour at a cylindrical structure. Archival Material, University of Florida, Book
3. Gotvald AJ, McCallum BE (2010) Epic flooding in Georgia
4. Khosronejad A, Diplas P, Angelidis D, Zhang Z, Heydari N, Sotiropoulos F (2020) Scour depth prediction at the base of longitudinal walls: a combined experimental, numerical, and field study. Environ Fluid Mech 20:459–478
5. Chaudhuri S, Singh S, Debnath K, Manik M (2018) Pier scour within long contraction in cohesive sediment bed. Environ Fluid Mech 18:417–441
6. Coleman SE (2005) Clearwater local scour at complex piers. J Hydraul Eng 131(4):330–334
7. Ettema R, Kirkil G, Muste MV (2006) Similitute of large-scale turbulence in experiments on local scour at cylinders. J Hydraul Eng 132(1):33–40
8. Melville BW (1997) Pier and abutment scour: integrated approach. J Hydraul Eng 123(2):125–136
9. Melville BW, Chiew YM (1999) Time scale for local scour at bridge piers. J Hydraul Eng 125(1):59
10. Oliveto G, Hagger WH (2002) Temporal evolution of clear-water pier and abutment scour. J Hydraul Eng 128(9):811–820
11. Raudkivi AJ, Ettema R (1983) Clear-water scour at cylindrical piers. J Hydraul Eng 109(3):338–350
12. Sheppard DM, Odeh M, Glasser T (2004) Large scale clear-water local pier scour experiments. J Hydraul Eng 130(10):957–963
13. Hong S, Sturm T, Stoesser T (2015) Clear water abutment scour in a compound channel for extreme hydrologic events. J Hydraul Eng 141(6):1–12
14. Hong S, Lee SO (2018) Insight of bridge scour during extreme hydrologic events by laboratory model studies. KSCE J Civ Eng 22(8):12871–12879
15. Lee SO, Hong S (2019) Turbulence characteristics before and after scour upstream of a scaled-down bridge pier model. Water 11(1900):1–14

16. Pu J, Lim SY (2014) Efficient numerical computation and experimental study of temporally long equilibrium scour development around abutment. Environ Fluid Mech 14:69–86
17. Keshavarzi A, Melville B, Ball J (2014) Three-dimensional analysis of coherent turbulent flow structure around a single circular bridge pier. Environ Fluid Mech 14:821–847
18. Bauri K, Sarkar A (2019) Turbulent burst-sweep events around fully submerged vertical square cylinder over plane bed. Environ Fluid Mech 19:645–666
19. Durafour M, Jarno A, Le Bot S, Lafite R, Marin F (2015) Bedload transport for heterogeneous sediments. Environ Fluid Mech 15:731–751
20. Carstens MR (1966) "Similarity laws for localized scour." American Society of Civil Engineers Proceedings. J Hydraul Div 92(HY3):13
21. Shen HW, Schneider VR, Karaki SS (1969) Local scour around bridge piers. J Hydraul Div 95(HY6):1919–1940
22. Torsethaugen K (1975) Lokal erosjon ved store konstruksjoner modellforsok. Vassdrags-og Havne-laboratoriet, Trondheim
23. Cunha LV (1975) Time evolution of local scour. In: Proceedings 16th congress, IAHR, Sao Paulo, Braz, pp 285–299
24. Zanke U (1982) Kolke am Pfeiler in richtungskonstanter Strömung und unter Welleneinfluß. Mitteilungen desFranzius-Instituts für Wasserbau-und Küsteningenieurwes. der Univ. Hann. 54:381–416
25. Pizarro A, Manfreda S, Tubaldi E (2020) The science behind scour at bridge foundations: a review. Water 12(374):1–26
26. Dey S (1999) Time-variation of scour in the vicinity of circular piers. Proc Inst Civ Eng Water Marit Energy 136:67–75
27. Ettema R (1980) Scour at bridge piers. No. 216, Dept. of Civil Engineering, University of Auckland, Auckland, New Zealand
28. Graf WH (1995) Local scour around piers. In: Lausanne EPFD (ed) Annual report, Laboratoire de Recherches Hydrauliques, Lausanne, Switzerland, B.33.1–B.33.8
29. Oliveto G, Hager WH (2005) Further results to time-dependent local scour at bridge elements. J Hydraul Eng 131(2):97–105
30. Kothyari U, Hager WH, Oliveto G (2007) Generalized approach for clear-water scour at bridge foundation elements. J Hydraul Eng 133(11):1229–1240
31. Chang W, Lai J, Yen C (2004) Evolution of scour depth at circular bridge piers. J Hydraul Eng 130(9):905–913
32. Kothyari U, Kumar A (2012) Temporal variation of scour around circular compound piers. J Hydraul Eng 138(11):945–957
33. Lanca R, Fael C, Maia R, Pego J, Cardoso A (2013) Clear-water scour at comparatively large cylindrical piers. J Hydraul Eng 139(11):1117–1125
34. Yao W, An H, Draper S, Cheng L, Harris J (2018) Experimental investigation of local scour around submerged piles in steady current. Coast Eng 142:27–41
35. Pandey M, Sharma PK, Ahmad Z, Singh UK (2018) Experimental investigation of clear-water temporal scour variation around bridge pier in gravel. Environ Fluid Mech 18:871–890
36. Link O, Castillo C, Pizarro A, Rojas A, Ettmer B, Escauriaza C, Manfreda S (2017) A model of bridge pier scour during flood waves. J Hydraul Res 55(3):310–323
37. Pizarro A, Samela C, Fiorentino M, Link O, Manfreda S (2017) BRISENT: an entropy-based model for bridge-pier scour estimation under complex hydraulic scenarios. Water 9(889):1–22
38. Raudkivi AJ (1986) Functional trends of scour at bridge piers. J Hydraul Eng 112(1):1–13
39. Sheppard DM, Miller W (2006) Live-bed local pier scour experiments. J Hydraul Eng 132(7):1–7
40. Melville BW, Sutherland AJ (1988) Design method for local scour at bridge piers. J Hydraul Eng 114(10):1210–1226
41. Melville BW, Coleman SE (2000) Bridge Scource. Water Resources Publication, Highlands Ranch
42. Lee SO, Sturm TW (2009) Effect of sediment size scaling on physical modeling of bridge pier scour. J Hydraul Eng 135(10):793–802
43. Ferraro D, Tafarojnoruz A, Gaudio R, Cardoso AH (2013) Effects of pile cap thickness on the maximum scour depth at a complex pier. J Hydraul Eng 139(5):482–491
44. Moreno M, Maia R, Couto L (2015) Effects of relative column width and pile-cap elevation on local scour depth around complex piers. J Hydraul Eng 142(2):1–9
45. Yang Y, Melville BW, Sheppard DM, Shamseldin AY (2018) Clear-water local scour at skewed complex bridge piers. J Hydraul Eng 144(6):1–10
46. Gautam P, Edlho TI, Mazumder BS, Behera MR (2019) Experimental study of flow and turbulence characteristics around simple and complex pier using PIV. Exp Therm Fluid Sci 100(2019):193–206

47. Keshavarzi A, Shrestha C, Melville B, Khabbaz H, Ranjbar-Zahedani M, Ball J (2018) Estimation of maximum scour depths at upstream of front and rear piers for two in-line circular columns. Environ Fluid Mech 18:537–550

48. Roulund A (2000) Three-dimensional numerical modelling of flow around a bottom-mounted pile and its application to scour. Department of Hydrodynamics and Water Resources, Technical University of Denmark, Lyngby, Denmark

49. Roulund A, Sumer BM, Fredsoe J, Michelsen J (2005) Numerical and experimental investigation of flow and scour around a circular pile. J Fluid Mech 534:351–401

50. Sturm TW (2006) Scour around Bankline and Setback Abutments in compound channels. J Hydraul Eng 132(1):21–32

51. Hong S, Abid I (2019) Scour around an erodible abutment with riprap apron over time. J Hydraul Eng 145(6):1–6

52. Sturm TW, Sotiropoulos F, Landers MN, Gotvald T, Lee S, Ge L, Navarro R, Escauriaza C (2004) Laboratory and 3D numerical modeling with field monitoring of regional bridge scour in Georgia. 2002, Georgia Department of Transportation, Atlanta, GA

53. Lee SO, Hong SH (2018) Reproducing field measurements using scaled-down hydraulic model studies in a laboratory. Adv Civ Eng 2018:9091506

54. Jones JS, Kilgore RT, Mistichelli MP (1992) Effects of footing location on bridge pier scour. J Hydraul Eng 118(2):280–290

55. Melville BW, Raudkivi AJ (1996) Effects of foundation geometry on bridge pier scour. J Hydraul Eng 122(4):203–209

56. Pizarro A, Ettmer B, Manfreda S, Rojas A, Link O (2017) Dimensionless effective flow work for estimation of pier scour caused by flood waves. J Hydraul Eng 143(7):635–642

57. Choo H, Zhao Q, Burns S, Sturm T, Hong S (2020) Laboratory and theoretical evaluation of impact of packing density, particle shape, and uniformity coefficient on erodibility of coarse-grained soil particles. Earth Surf Profess Landf 45(7):1499–1509

58. Dargahi B (1989) Turbulent flow field around a circular cylinder. Exp Fluids 8(1–2):1–12

59. Muzzammil M, Gangadhariah T (2003) Caracteristiques moyennes d'un vortex en fer a cheval au droit d'une pile cylindrique(The mean characteristics of horsehoe vortex at a cylindrical pier). J Hydraul Res 41(3):285–297

60. Lee SO (2006) Physical modeling of local scour around complex bridge piers. PhD thesis, Georgia Institute of Technology, Atlanta, GA

61. Link O, Henriquez S, Ettmer B (2019) Physical scale modelling of scour around bridge piers. J Hydraul Res 57(2):227–237

Publisher's Note　Springer Nature remains neutral with regard to jurisdictional claims in published maps and institutional affiliations.

Affiliations

Seung Oh Lee[1] · Irfan Abid[2] · Seung Ho Hong[3] 🔵

> Seung Oh Lee
> seungoh.lee@hongik.ac.kr

> Irfan Abid
> Irfan.abid@mce.nust.edu.pk

[1]　School of Urban and Civil Engineering, Hongik University, 94 Wausan-ro, Mapo-gu, Seoul 04066, Korea

[2]　Military College of Engineering, Risalpur, National University of Sciences and Technology, Islamabad, Pakistan

[3]　Department of Civil and Environmental Engineering, West Virginia University, 1306 Evansdale Drive, Morgantown, WV 26506, USA